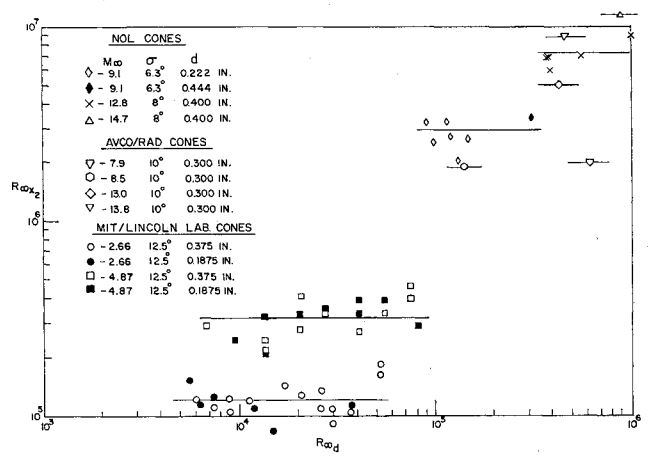

Fig. 5 Correlation of fully turbulent wake transition Reynolds number.

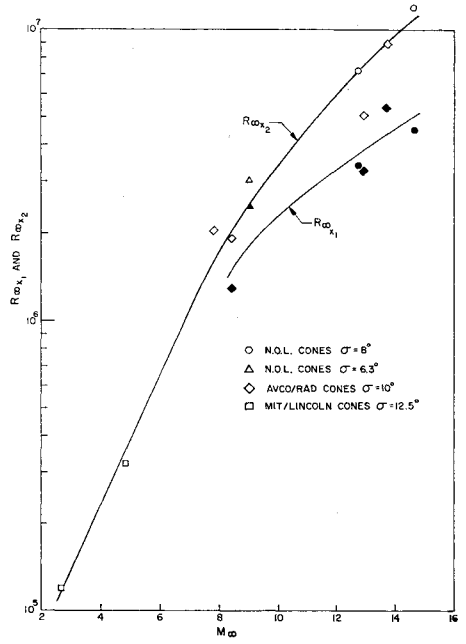

Fig. 6 Effect of freestream Mach number on wake transition Reynolds numbers.

The existence of a constant transition Reynolds number, independent of body diameter, was mentioned by Lees[6] in his description of a hypersonic wake flow model. From a correlation of blunt body wake transition data, Demetriades and Gold found a similar result.[7, 8]

The values of both wake transition Reynolds numbers $R_{\omega x_1}$ and $R_{\omega x_2}$ as functions of the freestream Mach number are shown in Fig. 6. The solid symbols represent the incipient transition Reynolds numbers, and the open symbols represent the fully turbulent ones. It appears that the transition zone of the viscous core increases in length with an increase of the freestream Mach number.

References

[1] Townsend, A. A., *The Structure of Turbulent Shear Flow* (Cambridge University Press, Cambridge, England, 1956), Chap. VII, pp. 169–171.

[2] Lyons, W. C., private communication, Naval Ordnance Lab. (1963).

[3] Hromas, L. and Lees, L., "Effect of nose bluntness on the turbulent hypersonic wake," Space Technology Labs. Rept. 6130-6259-KU-000 (October 1962).

[4] Slattery, R. E. and Clay, W. G., "The turbulent wake of hypersonic bodies," ARS Preprint 2673-62 (1962).

[5] Pallone, A. J., Erdos, I. I., Eckerman, J., and McKay, W., "Hypersonic laminar wakes and transition studies," AIAA Preprint 63-171 (1963).

[6] Lees, L., "Hypersonic wakes and trails," ARS Preprint 2662-62 (1962).

[7] Demetriades, A. and Gold, H., "Transition to turbulence in the hypersonic wake of blunt-bluff bodies," ARS J. **32**, 1420–1421 (1962).

[8] Demetriades, A. and Gold, H., "Correlation of blunt-bluff body wake transition data," Graduate Aeronaut. Lab., Calif. Inst. Tech. Internal Memo. 12 (September 1962).

Shock Curvature Effect on the Outer Edge Conditions of a Laminar Boundary Layer

IRVING RUBIN*
Republic Aviation Corporation, Farmingdale, N. Y.

Nomenclature

C_D = drag coefficient of spherical segment
$f(\eta)$ = dimensionless stream function
R = nose radius of the body
r = radial coordinate of the body
Re_R = Reynolds number based on nose radius
s = coordinate along the body surface
u = velocity
x = coordinate along the body axis of symmetry
y = radial coordinate of the shock wave
δ = boundary-layer thickness
θ_c = cone half-angle
θ_{sh} = local shock-wave angle
μ = absolute viscosity
ρ = density
ψ = stream function

Subscripts

∞ = freestream condition
e = condition at outer edge of boundary layer

PREDICTION techniques for aerodynamic heating are dependent on the boundary-layer outer edge conditions. The method by which these conditions are obtained will therefore influence the magnitude of the computed heat-transfer rates. Thus, consider the region of simple blunted shapes several nose diameters or more downstream of the stagnation point. The boundary-layer outer edge conditions may be obtained here by either assuming an attached shock wave or by expanding isentropically from the normal shock conditions at the nose stagnation point to the known local pressure. The resulting heat-transfer rates will be quite different depending on the method used.

Since the first method applies far downstream of the stagnation region and the second method applies in the vicinity of the nose or leading edge, there exists a substantial region along the body where the outer edge conditions, and hence the heating rates, are intermediate to the forementioned two extremes.

A method for determining the variation of the flow conditions at the outer edge of a laminar boundary layer over a blunted cone resulting from entropy gradients due to shock wave curvature is presented in Ref. 1. The method is derived for a perfect gas, and the reported results were obtained using an electronic computer.

The purpose of this note is to point out a simple approach for solving this problem graphically, which includes real gas effects, and to indicate the effect resulting from the perfect gas assumption in the hypersonic flow regime.

Received August 23, 1963.

* Principal Thermodynamics Engineer, Paul Moore Research and Development Center. Member AIAA.

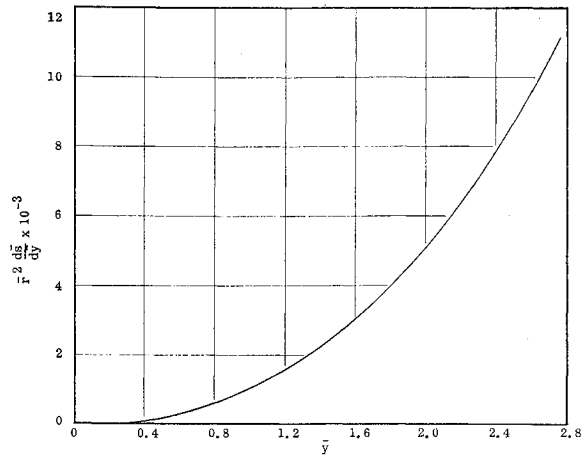

Fig. 1 Variation of the parameter $\bar{r}^2 d\bar{s}/d\bar{y}$ with the shock-wave coordinate $\bar{y}$; $R = 6$ in.

Consider a streamline that crosses the bow shock wave at a point y and subsequently enters the laminar boundary layer at the point s along the body surface. A balance of the mass flow within that streamtube between the free-stream conditions and the conditions within the boundary layer can be represented as

$$y^{j+1}\rho_\infty u_\infty = 2^j \psi(s,\delta) \tag{1}$$

where $j = 0$ for two-dimensional flow and $j = 1$ for axisymmetric flow. The stream function ψ is, assuming similarity,

$$\psi(s,\delta) = \int_0^\delta \rho u r^j dy = (2\bar{s})^{1/2} f(\eta_\delta) \tag{2}$$

where

$$\bar{s} = \int_0^s \rho_e u_e \mu_e r^{2j} ds \tag{3}$$

Combining Eqs. (1–3) and nondimensionalizing all lengths with respect to R and all flow parameters with respect to their corresponding freestream values yields the following relation:

$$\bar{r}^{2j}\frac{d\bar{s}}{d\bar{y}} = \frac{2(j+1)}{[f(\eta_\delta)]^2}\left(\frac{\bar{y}}{2}\right)^{2j+1}\frac{Re_{\infty R}}{\bar{\rho}_e \bar{u}_e \bar{\mu}_e} \tag{4}$$

where the barred quantities are nondimensionalized as indicated.

Equation (4) represents a relation between the shock wave coordinate y and the body physical coordinate s with a dependence on the flow parameters at the outer edge of the boundary layer. The solution of this equation may be obtained quite simply through a graphical integration involving no iterations for the particular case of a zero pressure gradient along the body. This is generally the case, because the streamline that crosses the shock wave quite close to the stagnation point enters the boundary layer at a point s along the body where the pressure has already attained its asymptotic value. Furthermore, it was shown in Ref. 1 and also observed in the present study that the initial pressure variation along the body prior to attaining its constant asymptotic value has only a local and negligibly small downstream effect on the computed flow parameters.

In order to illustrate the use of Eq. (4) in obtaining the boundary-layer outer edge conditions, consider a spherically blunted cone ($\theta_c = 15°$) at Mach 20 and an altitude of 150,000 ft. An expression for the shock shape, successfully correlated in Ref. 2 in terms of the blast wave parameters, is

$$\frac{\bar{y}}{\cos\theta_c} = 1.424\left(C_D^{1/2}\frac{\bar{x}}{\cos\theta_c}\right)^{0.46} \tag{5}$$

which fares into the conical shock wave. From Eq. (5), the local shock wave angle is

$$\tan\theta_{sh} = 0.992\, C_D^{1/2}(\cos\theta_c/\bar{y})^{1.174} \tag{6}$$

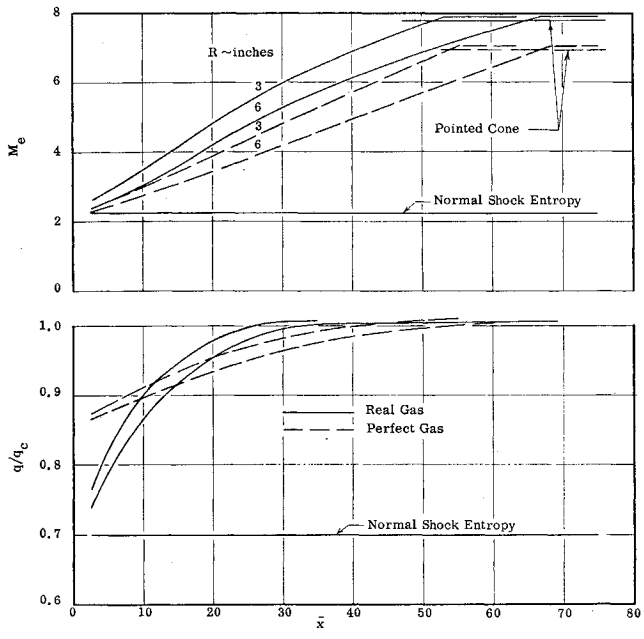

Fig. 2 Distribution of local Mach number and heat-transfer rate along blunted cone; $\theta_c = 15°$, $M_\infty = 20$, alt = 150,000 ft.

Thus, for a particular shock wave angle that corresponds to an assumed value of $\bar{y}$, all the properties immediately behind the shock wave are known from the oblique shock relations. Expansion of these conditions isentropically (along a streamline) using a Mollier diagram to the cone surface pressure, as given by the attached conical shock wave solution or by modified Newtonian flow theory, will define the boundary-layer outer edge conditions at some station s, as yet unknown. These outer-edge parameters may now be used in Eq. (4) to calculate the value of $\bar{r}^2 d\bar{s}/d\bar{y} = F(\bar{y})$. Repeating the foregoing procedure for several values of $\bar{y}$ will yield the curve of Fig. 1. The area under the curve for any value of $\bar{y}$ is therefore

$$\int_0^{\bar{s}} \bar{r}^2 d\bar{s} = \int_0^{\bar{y}} F(\bar{y}) d\bar{y}$$

and, since

$$\bar{r} = \cos\theta_c + [\bar{s} + \theta_c - (\pi/2)]\sin\theta_c \tag{7}$$

the resulting equation for $\bar{s}$ becomes

$$\bar{s}^3 + 3[\cot\theta_c + \theta_c - (\pi/2)]\bar{s}^2 + 3[\cot\theta_c + \theta_c - (\pi/2)]^2\bar{s} = \frac{3}{\sin^2\theta_c}\int_0^{\bar{y}} F(\bar{y})d\bar{y} \tag{8}$$

The value of $\bar{s}$ is then the positive root of the foregoing cubic equation.

The local Mach number variation along the cone surface, determined in the manner just described, is presented in Fig. 2 for both a real and perfect gas and for two values of the nose radius. The real gas effect is seen to be quite significant for that flight condition. Also shown in Fig. 2 is the heat-transfer rate along the cone surface nondimensionalized with respect to the pointed conical value. This heat-transfer ratio is seen to approach its asymptotic value considerably faster than the Mach number. Furthermore, the assumption of normal shock entropy appears to be overly optimistic. The effect of the perfect gas assumption on heat transfer is seen to be initially conservative, and it becomes optimistic beyond a distance along the cone surface of approximately 11–15 nose radii.

References

[1] Zakkay, V. and Krause, E., "Boundary conditions at the outer edge of the boundary layer on blunted conical bodies," Aeronaut. Res. Labs. 62-386 (July 1962).

[2] Klaimon, J. H., "Bow shock correlation for slightly blunted cones," AIAA J. 1, 490–491 (1963).

Linear Programming for Life Support Optimization

NEIL W. O'ROURKE*

General Dynamics/Astronautics, San Diego, Calif.

Nomenclature

b_i = ith life support requirement, lb/man-day
x_j = installed weight of the jth life support process, lb
a_{ji} = pounds per day input or output of the ith material, produced by one installed pound of the jth process
W = total weight chargeable to life support system, including effect on radiator weight, lb
c_j = total weight chargeable to jth process, including effect on radiator weight, pounds per installed pound of the jth process

Introduction

LINEAR programming is used to optimize the design and operation of a chemical plant operating with different raw materials, intermediate materials, products, and forms of energy.[1] In this paper linear programming is used to optimize the air, water, and thermal control for a one man-day life support system based on the storage of supplies and wastes. A similar approach could be used to minimize cost or optimize for some other desirable condition for the various types of environmental control systems.

Analysis

The requirements for thermal, atmosphere, and water management for one man-day are listed in Table 1. It is assumed that water vapor is condensed and re-used, and the daily water requirement is reduced accordingly.

Different processes can be selected to provide for the requirements in Table 1. The processes considered in this paper are listed in Table 2, along with the coefficients relating each process with the environmental requirements [Eq. (1)] and with the weight W that is to be minimized [Eq. (2)]:

$$b_i = \sum_j a_{ji}x_j \qquad (1)$$

$$W = \sum_j c_j x_j \qquad (2)$$

The values shown are presented as typical only and will vary with the exact formulation of each process and the equipment and operating techniques used. The relations are assumed linear as an approximation. Since some of the processes release or absorb more than one material, there are various cross terms. The coefficient that shows the effect of KO_2 on the water balance is negative, $a_{5,2} = -0.16$, because water is absorbed when KO_2 absorbs CO_2 and releases O_2. The coefficient c_j (defined in Table 2) accounts for the required change in radiator weight due to a unit change in the weight of process x_j. For instance, liquid oxygen absorbs heat and reduces radiator weight; therefore, $c_1 = 0.92$. Hydrogen peroxide, on the other hand, releases heat, and $c_2 = 1.59$.

Where there are two more variables than constraints, a plot of the problem can be made on a two-dimensional graph,

Received July 22, 1963; revision received August 26, 1963.

* Preliminary Design Engineer, Space Station Program. Member AIAA.

Table 1 Life support requirements, lb/man-day

Substance	Quantity	Symbol
Oxygen input	2	b_1
Water input	2.8 (net)	b_2
Carbon dioxide output	2.3	b_3

Table 2 Programming data

Agent	Programming variable	Pertinent coefficients
$O_2(l)$	x_1	$a_{1,1} = 0.8$; $c_1 = 0.92$
H_2O_2	x_2	$a_{2,1} = 0.36$; $a_{2,2} = 0.5$; $c_2 = 1.59$
H_2O	x_3	$a_{3,2} = 0.9$; $c_3 = 1.0$
LiOH	x_4	$a_{4,3} = 0.8$; $a_{4,2} = 0.33$; $c_4 = 1.57$
KO_2	x_5	$a_{5,1} = 0.29$; $a_{5,2} = -0.16$; $a_{5,3} = 0.27$; $c_5 = 1.34$

and the optimum can be found by inspection (see Fig. 1). The lines are determined by solving for the weight in terms of x_2 and the other variables, individually, in succession. The other variable is then set equal to zero, and the various straight lines can be plotted.

Thus, in Fig. 1, the vertical axis represents the total weight, and the horizontal axis represents the weight of hydrogen peroxide and hydrogen peroxide storage equipment. Along the vertical axis the amount of hydrogen peroxide is zero. The various straight lines on the figure represent points where the weight of the process noted is zero. On one side of these lines the weight would be negative, and these sides are excluded as shown by the hatching.

The only allowed solutions are those represented by points within the shaded area. Since the vertical axis represents the weight that is to be minimized, the optimum is represented by the lowest point within the shaded area. This point is on the intersection of the lines where hydrogen peroxide and potassium superoxide are both zero. The nonzero substances are water, liquid oxygen, and lithium hydroxide. These substances would be used in the life support system. The total weight would be a little under 9 lb.

The more general method of solving linear programming problems involves the use of "tableaux." Only a sketch of the method can be given here (see Ref. 2 for details). The basic idea is the same as in the graphical solution. Since the relations are linear, the allowed solutions will represent a convex set in a space with dimensions equal to the variables minus the constraints. This means that there are no "re-entrant ridges," and, if water were placed in a vessel

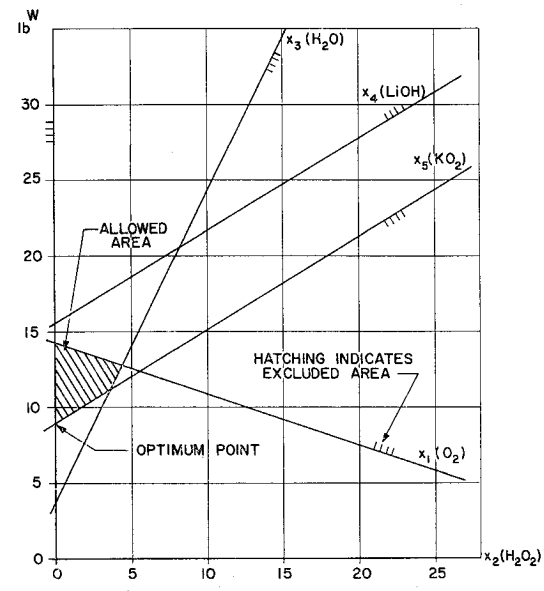

Fig. 1 Graphical solution of linear programming.